

## Precision Measurement of the Magnetic Moment of the $\Sigma^-$ Hyperon

D. W. Hertzog,<sup>(a)</sup> M. Eckhause, K. L. Giovanetti,<sup>(b)</sup> J. R. Kane, W. C. Phillips, W. F. Vulcan,  
R. E. Welsh, R. J. Whyley, and R. G. Winter

*College of William and Mary, Williamsburg, Virginia 23185*

and

G. W. Dodson,<sup>(c)</sup> J. P. Miller, F. O'Brien, B. L. Roberts, and D. R. Tieger

*Boston University, Boston, Massachusetts 02215*

and

R. J. Powers

*California Institute of Technology, Pasadena, California 91125*

and

N. J. Colella and R. B. Sutton

*Carnegie-Mellon University, Pittsburgh, Pennsylvania 15213*

and

A. R. Kunselman

*University of Wyoming, Laramie, Wyoming 82071*

(Received 31 May 1983)

The magnetic moment of the  $\Sigma^-$  hyperon has been obtained from measurements of fine-structure splittings of x-ray transitions in  $\Sigma^-$  exotic atoms. The use of targets consisting of sheets of Pb or W immersed in liquid hydrogen, and of a tagging technique utilizing the  $\pi^+$  emitted in the reaction  $K^-p \rightarrow \Sigma^- \pi^+$ , resulted in improved x-ray signal-to-noise ratio by a factor of 15 over that in previous experiments. The present result is  $\mu(\Sigma^-) = (1.111 \pm 0.031 \pm 0.011)\mu_N$ .

PACS numbers: 14.20.Jn, 13.40.Fn, 36.10.Gv

Simple models<sup>1,2</sup> which combine Dirac moments of individual quarks via SU(6) have been used in the past with qualitative success to relate the magnetic moments for members of the spin- $\frac{1}{2}$  baryon octet. Currently, corrections to the models<sup>3</sup> are required to produce agreement with new experimental values<sup>4-8</sup> for some of these moments. Since earlier measurements<sup>9,10</sup> of the  $\Sigma^-$  moment  $\mu(\Sigma^-)$  were not of sufficient precision to test the more recent models, we have remeasured  $\mu(\Sigma^-)$  with an improved version of the exotic-atom technique. This work has resulted in a more precise value for the fine-structure splittings of  $\Sigma^-$  atomic x rays from which  $\mu(\Sigma^-)$  may be determined.

The apparatus used in the present experiment is shown schematically in Fig. 1. Kaons of 680 MeV/c from the C4 beam at the Brookhaven National Laboratory alternating gradient synchrotron (AGS) were brought to rest in a laminar target assembly which consisted of nineteen sheets of a target metal (0.4 g/cm<sup>2</sup> Pb or W) spaced 5 mm apart in a liquid-hydrogen vessel. The sheets were 15 cm long and ranged in height from 10.5

cm in the center to 6.5 cm at the sides. The  $\Sigma^-$  produced in the hydrogen by the reaction



were tagged by detection of the 83-MeV  $\pi^+$ . This reaction occurs with a branching ratio of 44% and generates  $\Sigma^-$  with a kinetic energy of 12.4 MeV. A large fraction of these survived decay and were brought to rest in the adjacent target sheets.

The beam contained 10%  $K^-$  which were selected by a Cherenkov counter and by a  $dE/dx$  threshold on  $S_5$ . Range scintillation spectrometers ( $\pi R$  and  $\pi L$  in Fig. 1) were placed on each side of the target to detect the  $\pi^+$  produced in Reaction (1). The aluminum-degrader thickness was adjusted to maximize  $\pi^+$  stops in the central element of three  $46 \times 46 \times 2.5$ -cm<sup>3</sup> plastic-scintillation counters. The stopped  $\pi^+$  were identified by the subsequent detection of the positron from the decay chain  $\pi^+ \rightarrow \mu^+ \rightarrow e^+$ .

X rays from  $\Sigma^-$  atoms were detected in three intrinsic reverse-electrode Ge detectors which were housed in a single cryostat located below the target. A stopped  $K^-$  in coincidence with a

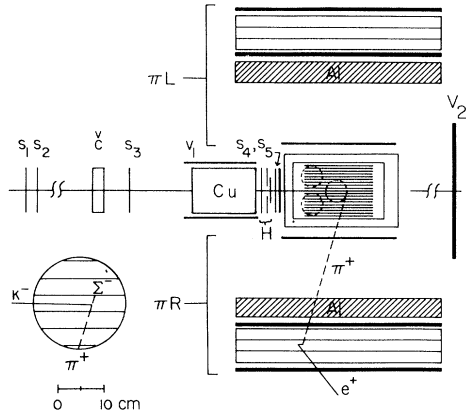


FIG. 1. Experimental arrangement.  $S_1$ - $S_5$  are beam-defining scintillation counters;  $V_1$  is a veto counter surrounding the Cu moderator;  $V_2$ , a downstream veto counter;  $H$ , a beam-defining hodoscope;  $\pi L$  and  $\pi R$ , pion spectrometers including Al moderator; and  $C$ , a Cherenkov counter to detect kaons. The laminar target assembly is shown with three Ge detectors located below. Inset: a typical  $K^-p$  interaction in the region between target sheets.

Ge detector signal formed the event trigger for "untagged" x-ray spectra. If, in addition, a  $\pi^+$  signature from either of the  $\pi^+$  range spectrometers accompanied the x ray, the event was labeled "tagged."

The relatively large  $\Sigma^-$  yield and the tagging of its production have resulted in an enhancement of 15:1 in x-ray signal-to-noise ( $S/N$ ) ratio over that of previous experiments.<sup>9,10</sup> Displayed in Fig. 2 is a portion of the tagged and untagged spectra obtained in the present work. These spectra clearly show substantial improvement in  $S/N$  for the tagged  $\Sigma^-Pb(12-11)$  x-ray peak and the suppression of a nearby background kaonic-atom x-ray peak. For the tagged  $\Sigma^-Pb(11-10)$ ,  $\Sigma^-Pb(12-11)$ , and  $\Sigma^-W(11-10)$  data which were used in this measurement  $S/N$  values were 3:1 or larger.

Ge-detector-calibration data were obtained throughout the experiment in two modes which exploited the AGS 2.8-s beam cycle. During beam-on periods, events were accepted which consisted of the random coincidences between  $\gamma$  rays from radioactive sources (positioned between target and detector) and a logic gate opened when a beam  $\pi^-$  or  $\mu^-$  entered the target. These data were used to obtain the instrumental resolution and line shape as a function of energy for each detector under beam-on conditions. The experimental line shape was well represented by a Gaussian function. Between beam pulses, his-

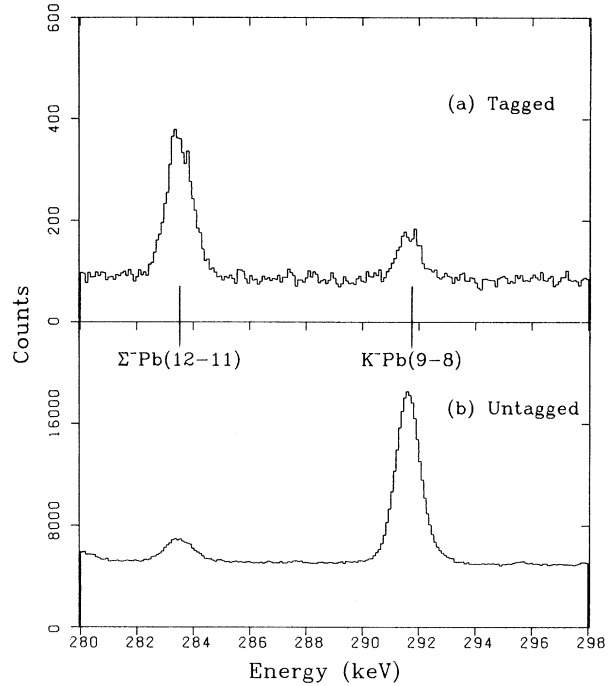


FIG. 2. (a) "Tagged" x-ray spectrum, showing the  $\Sigma^-Pb(12-11)$  transition and the nearby  $K^-Pb(9-8)$  transition. (b) The "untagged" x-ray spectrum for the same energy region. While the  $S/N$  for the  $\Sigma^-Pb(12-11)$  transition is better than that in earlier  $\Sigma^-$  exotic-atom experiments, it is substantially worse than in the tagged mode.

tograms of two  $\gamma$ -ray lines near the end points of the energy spectrum were formed. These histograms were written to tape every 10 min. Least-squares fits which determined the centroids of these histograms were used to form the basis of an off-line two-point stabilization routine used in the data analysis.

The fine-structure splitting of a  $\Sigma^-$  atomic level with principal quantum number  $n$ , orbital quantum number  $l$ , and nuclear charge  $Z$  is given approximately by<sup>11</sup>

$$\Delta E_{nl} = (g_0 + 2g_1)(Z\alpha)^4 mc^2 / 2n^3 l(l+1), \quad (2)$$

where  $m$  is the  $\Sigma^-$ -nucleus reduced mass,  $\alpha$  is the fine-structure constant, and  $g_0 = -1$  is the Dirac part and  $g_1$  the anomalous (Pauli) part of the magnetic moment. The magnetic moment can be written as

$$\mu(\Sigma^-) = (g_0 + g_1) e\hbar / 2m_\Sigma = (g_0 + g_1)(m_p/m_\Sigma)\mu_N,$$

where  $\mu_N$  is the nuclear magneton and  $m_p$  and  $m_\Sigma$  are the  $p$  and  $\Sigma^-$  masses.

The relative intensities of the components within a fine-structure x-ray doublet have been calculated for a statistical population of the  $l \pm \frac{1}{2}$  an-

gular momentum states.<sup>11</sup> At high  $n$  there are only two observable lines and the intensity largely arises from transitions between "circular" orbits (those with  $l = n - 1$ ). These two components were separated in energy by less than the instrumental resolution. The observed peak was therefore a broadened structure composed principally of two single Gaussians. Additionally, in the fitting procedure, low-intensity transitions between noncircular orbits ( $l \leq n - 2$ ) had to be taken into account because, although different in energy, they are unresolved from the transitions between circular orbits.

Atomic cascade calculations were carried out to determine the noncircular contributions to each doublet. The initial populations of states in the cascade calculations were constrained by our measurements of six  $\Delta n = 1$  and three  $\Delta n = 2$  transitions for Pb, and five  $\Delta n = 1$  and two  $\Delta n = 2$  transitions for W. An optical potential<sup>12</sup> was used to estimate the strong-interaction absorption from each level. The initial populations and the imaginary part of the strong-interaction scattering length were varied and the calculated intensities were compared with the data. Minimization of  $\chi^2$  in this procedure determined the best model for the cascade process. The ratios of the intensities of total noncircular to circular transitions were found to be  $0.022 \pm 0.005$  for the  $\Sigma^- \text{Pb}(11-10)$  transition,  $0.122 \pm 0.024$  for the  $\Sigma^- \text{Pb}(12-11)$  transition, and  $0.120 \pm 0.020$  for the  $\Sigma^- \text{W}(11-10)$  transition.

Fits of the  $\Sigma^-$  x-ray peaks in the tagged data were made for each detector. In each fit the two circular components, the two  $l = n - 2$  noncircular components, and a three-parameter polynomial background were included. Each of the four transition components was represented by a single Gaussian of the same instrumental width. For the  $\Sigma^- \text{Pb}(11-10)$  transition at 373 keV, the strong-interaction line shape ( $23 \pm 7$  eV full width at half maximum) was convoluted with the instrumental line shape (typically  $1100 \pm 7$  eV full width at half maximum). The relative amplitudes of the components were fixed as discussed above. Although Eq. (2) contains the essential features of the  $g_1$  dependence of the splitting, it was not used directly to determine  $\mu(\Sigma^-)$ . Rather all level energies (circular and noncircular) were completely calculated as a function of  $g_1$ . This involved corrections<sup>13</sup> to the Dirac energies for vacuum polarization, finite nuclear size, nuclear polarization, electron screening and recoil corrections to the vacuum polarization, anomalous

moment, and point Coulomb energies. Uncertainties in these corrections have a negligible effect on the final result compared to that of the experimental error. Consequently, the separations of all components in each peak were fixed uniquely for a given value of  $g_1$ . Least-squares fits to the data were made for a wide range of values for  $g_1$ , and the resulting  $\chi^2$  were plotted as a function of  $\mu(\Sigma^-)$ . From these  $\chi^2$  plots,  $\mu(\Sigma^-)$  and its statistical uncertainty were obtained for each transition.

Tests of this method for extracting the separation of the centroids of two, or four, Gaussians from a single broad structure were made. A large set of multiple Gaussian doublets for a wide range of assumed splittings and  $S/N$  was generated through standard computer simulation techniques. These simulations were then fitted with the routines used in the data analysis. Further tests using the entire x-ray spectroscopy system were made with radioactive sources with pairs of known  $\gamma$ -ray lines separated in energy by 330 and 580 eV, amounts similar to that expected for the  $\Sigma^-$  x-ray doublets. In both studies, analysis of the broadened structures yielded the correct separation of the individual peaks.

Our results complement those from precession experiments recently reported from Fermilab.<sup>7,8</sup> In the latter, polarized  $\Sigma^-$  are precessed in a magnetic field and the asymmetry in  $\Sigma^-$  decay is exploited to obtain the moment. The low value of the  $\Sigma^-$  asymmetry parameter ( $-0.068 \pm 0.008$ ) makes the precession measurement for  $\Sigma^-$  considerably more difficult than for other baryons. To determine the sign of  $\mu(\Sigma^-)$  by the exotic-atom method, it is necessary to measure the small difference in amplitude of the individual Gaussians<sup>9</sup> so as to determine whether the  $l + \frac{1}{2}$  or the  $l - \frac{1}{2}$  states are higher in energy. At present, neither experimental technique alone provides an unambiguous choice of the sign of the magnetic moment. However, as pointed out by Deck *et al.*,<sup>7</sup> only the negative values for  $\mu(\Sigma^-)$  among the three recent experiments are statistically consistent. Accordingly we limit the following discussion to the negative value obtained here.

In Fig. 3, we show the results of fits to the tagged  $\Sigma^- \text{Pb}(11-10)$ ,  $\Sigma^- \text{Pb}(12-11)$ , and  $\Sigma^- \text{W}(11-10)$  transitions for each of the three detectors. The uncertainties shown are statistical only and are equal to the changes in the values of the magnetic moment for which  $\chi^2$  changes by unity from the minimum. Summed  $\chi^2$  maps from all of the data treated here yield a  $\chi^2$  minimum of 2259 for

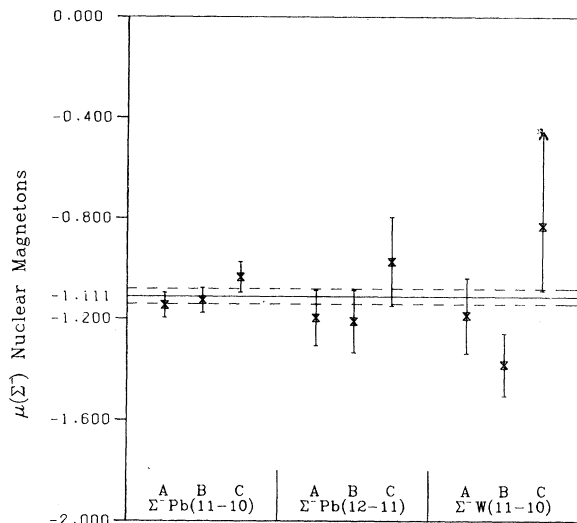


FIG. 3. The values for  $\mu(\Sigma^-)$  extracted from the  $\Sigma^- \text{Pb}(11-10)$ ,  $\Sigma^- \text{Pb}(12-11)$ , and  $\Sigma^- \text{W}(11-10)$  transitions in the tagged-data spectra. Values are shown for each Ge detector separately and the errors are statistical only.

2106 degrees of freedom whereas  $\chi^2$  for zero fine-structure splitting is 2406.

We have examined the sensitivity of the measured magnetic moment to the uncertainties in the following: instrumental resolution of the detectors, background shape in the region of fit, relative intensity of the components of the fine-structure doublets, strong-interaction widths, calculated energy levels, and the intensity of the non-circular components. An incorrect estimate of these last four contributions affects the consistency of results obtained from different transitions. The good agreement among the results presented in Fig. 3 indicates therefore that these contributions are understood. The systematic error due to all uncertainties is estimated to be  $\pm 0.011\mu_N$ . Hence, our combined result for all of the data is  $\mu(\Sigma^-) = (-1.111 \pm 0.031 \pm 0.011)\mu_N$ , where the first error is statistical only.

Quark calculations of baryon magnetic moments generally do not include effects such as configuration mixing, exchange corrections, and relativistic corrections which are estimated<sup>14</sup> to be 10%. Therefore, disagreements between theory and experiment at this level cannot be used as arguments against the basic validity of any theory. However, the present result is difficult to reconcile with the calculations of Brown, Rho, and Vento<sup>15</sup> and of González, Vento, and Rho,<sup>16</sup> which give  $\mu(\Sigma^-)$  values between  $-0.54\mu_N$  and  $-0.70\mu_N$ , and with the approach of Lipkin<sup>17</sup> which gives

$\mu(\Sigma^-) = -0.81\mu_N$ . Instead our result is in reasonable agreement with the simple-quark-model prediction<sup>1</sup> of  $\mu(\Sigma^-) = -1.05\mu_N$  and the cloudy-bag-model prediction<sup>3</sup> of  $\mu(\Sigma^-) = -1.09\mu_N$ .

We acknowledge the important efforts of R. Pehl, F. Goulding, D. Landis, and N. Madden of Lawrence Berkeley Laboratory and those of R. Trammell of EG&G Ortec in development of the detector array and associated electronics used in this work. We thank the AGS staff and the hydrogen target group of Brookhaven National Laboratory for their continued support. We are indebted to E. Borie for a computer program used to calculate electromagnetic corrections and to R. Seki and M. Leon for use of their hadronic cascade program. We thank T. Williams for valuable programming assistance. This work has been supported by the National Science Foundation and the Department of Energy. This work is based on a dissertation submitted by one of us (D.W.H.) to the College of William and Mary in partial fulfillment of the requirements for the Ph.D. degree.

<sup>(a)</sup>Present address: Carnegie-Mellon University, Pittsburgh, Pa. 15213.

<sup>(b)</sup>Present address: Swiss Institute for Nuclear Research, Ch-5234 Villigen, Switzerland.

<sup>(c)</sup>Present address: Massachusetts Institute of Technology, Cambridge, Mass. 02139.

<sup>1</sup>A. De Rujula, H. Georgi, and S. L. Glashow, *Phys. Rev. D* **12**, 147 (1975); J. Franklin, *Phys. Rev.* **172**, 1807 (1968), and **182**, 1607 (1969).

<sup>2</sup>T. DeGrand, R. L. Jaffee, K. Johnson, and J. Kiskis, *Phys. Rev. D* **12**, 2060 (1975).

<sup>3</sup>See, for example, S. Théberge and A. W. Thomas, *Nucl. Phys.* **A393**, 252 (1983), and references therein.

<sup>4</sup>L. Schachinger *et al.*, *Phys. Rev. Lett.* **41**, 1348 (1978).

<sup>5</sup>P. T. Cox *et al.*, *Phys. Rev. Lett.* **46**, 877 (1981).

<sup>6</sup>R. Settles *et al.*, *Phys. Rev. D* **20**, 2154 (1979).

<sup>7</sup>L. Deck *et al.*, *Phys. Rev. D* **28**, 1 (1983).

<sup>8</sup>J. Marriner *et al.*, in *High Energy Spin Physics—1982*, edited by G. Bunce, AIP Conference Proceedings No. 95 (American Institute of Physics, New York, 1983), p. 64; preliminary results.

<sup>9</sup>B. L. Roberts *et al.*, *Phys. Rev. D* **12**, 1232 (1975).

<sup>10</sup>G. Dugan *et al.*, *Nucl. Phys.* **A254**, 396 (1975).

<sup>11</sup>See, for example, H. A. Bethe and E. Salpeter, *Quantum Mechanics of One- and Two-Electron Atoms* (Academic, New York, 1957).

<sup>12</sup>C. J. Batty *et al.*, *Phys. Lett.* **74B**, 27 (1978).

<sup>13</sup>E. Borie, *Phys. Rev. A* **28**, 555 (1983).

<sup>14</sup>N. Isgur and G. Karl, *Phys. Rev. D* **21**, 3175 (1980).

<sup>15</sup>G. E. Brown, M. Rho, and V. Vento, *Phys. Lett.* **84B**, 383 (1979).

<sup>16</sup>P. González, V. Vento, and M. Rho, *Nucl. Phys.* **A395**, 446 (1983).

<sup>17</sup>H. Lipkin, *Nucl. Phys.* **B214**, 136 (1983).